

# Reservoir-engineered spin squeezing in quantum hybrid solid-state platforms

Jayakrishnan M. P. Nair<sup>1,\*</sup> and Benedetta Flebus<sup>1,†</sup>

<sup>1</sup>*Department of Physics, 140 Commonwealth Avenue, Chestnut Hill, Massachusetts 02467, USA*

(Dated: October 22, 2024)

Spin squeezing, a form of many-body entanglement, is a crucial resource in quantum metrology and information processing. While experimentally viable protocols for generating stable spin squeezing have been proposed in quantum-optical platforms using atomic ensembles, there is growing interest in quantum hybrid solid-state systems as alternative platforms for exploring many-body quantum phenomena. In this work, we propose a scheme to generate long-lived spin squeezing in an ensemble of solid-state qubits interacting with electromagnetic noise emitted by a squeezed solid-state bath. We identify the conditions under which quantum correlations within the bath can be transferred to the qubit array, effectively driving the qubits into an entangled state, regardless of their initial configuration. To assess the experimental feasibility of our approach, we investigate the dynamics of an array of solid-state spin defects coupled to a common ferromagnetic bath, which is driven into a non-equilibrium squeezed state through its interaction with a surface acoustic wave mode. Our results demonstrate that the ensemble can exhibit steady-state spin squeezing under suitable conditions, paving the way for the generation of steady-state many-body entanglement in ensembles of solid-state spin defects.

## I. INTRODUCTION

Central to the development of quantum technologies is the concept of squeezing, which characterizes the reduction of quantum uncertainty in one observable of a system at the expense of increased uncertainty in its conjugate observable. The generation of squeezed states has been explored in a broad variety of systems, including — but not limited to — Bose-Einstein condensates [1–14], optomechanical systems [15–19], mechanical systems [20, 21], and magnonic systems [22–27]. Among these squeezing realizations, a valuable resource for quantum metrology lies in spin squeezed states [28], which can be realized in systems that can be described by collective spin variables, such as the atomic ensembles [29–32] conventionally used in Ramsey spectroscopy [33, 34] and atomic clocks [30, 34, 35].

An essential property of spin squeezing is its direct relation with multi-partite entanglement, whose characterization and measurement remain otherwise elusive in many-body systems. The degree of spin squeezing can be quantified, among others [36], in terms of Wineland’s spin squeezing parameter  $\xi_R^2$  [34], which compares the quantum fluctuations in one spin component to those of a coherent spin state. Specifically, a value of  $\xi_R^2$  less than one indicates reduced quantum fluctuations and, for any many-body spin-1/2 state, signals the presence of entanglement [5].

Several proposals for generating spin squeezing in atomic ensembles rely on their interaction with a common squeezed photonic reservoir, which enables the transfer of squeezing from the light to the atoms. For instance, in the far-detuned regime, the coherent interactions between the atomic ensemble and a cavity mode result in an effective qubit-qubit Hamiltonian whose nonlinear twisting terms can be used to generate spin squeezing. Such one- and two-axes twisting Hamiltonians have been explored both theoretically [37, 38] and experimentally [39, 40] across various platforms. As for any

entanglement protocol relying on coherent qubit-qubit interactions, however, here the decoherence resulting from the dissipative interaction with the environment plays a detrimental role, shortening the lifetime of spin squeezed states.

An alternative route is offered by reservoir engineering approaches that turn dissipation into a resource for the generation and stabilization of a form of many-body quantum entanglement that is robust to variations in the system’s initial state [16, 41–51]. In these schemes, the squeezing properties of the bath are imparted to the system via its dissipative coupling to a nontrivial common environment, with an efficiency that increases with the size of the qubit ensemble. The dissipative preparation of many-body spin squeezed states has been proposed in several settings, e.g., involving direct driving with squeezed light [52–54], the use of Raman processes [41] in structured atoms, and the coupling to a bosonic mode that, in turn, interacts with a squeezed reservoir [42]. However, it still awaits experimental realization.

The central goal of this work is to transfer and adapt this approach to solid-state quantum hybrid platforms, consisting of an ensemble of solid-state spin defects interacting with a common magnetic bath, which, as we will demonstrate, can be driven into a squeezed state using already established experimental techniques. Due to their long coherence times and optical addressability, solid-state spin defects, such as nitrogen- or silicon-vacancy (NV, SiV) centers, have garnered considerable attention over the past decades as promising qubit platforms [55–57]. However, the generation of robust long-distance entanglement [58–61] among these qubits has proven experimentally challenging due to environment-driven decoherence, suggesting that reservoir engineering approaches may offer a viable alternative.

A first step in this direction was made by Li *et al.* [62], who derived a comprehensive formalism for the quantum many-body dynamics of an ensemble of solid-state spin defects interacting with a common solid-state reservoir. In this work, the authors investigate the strength of dissipation-driven quantum cooperative phenomena, such as superradiant and subradiant collective emission [63], by focusing on a stationary  $U(1)$ -symmetric magnetic bath. Here, we generalize this

\* muttathi@bc.edu

† flebus@bc.edu

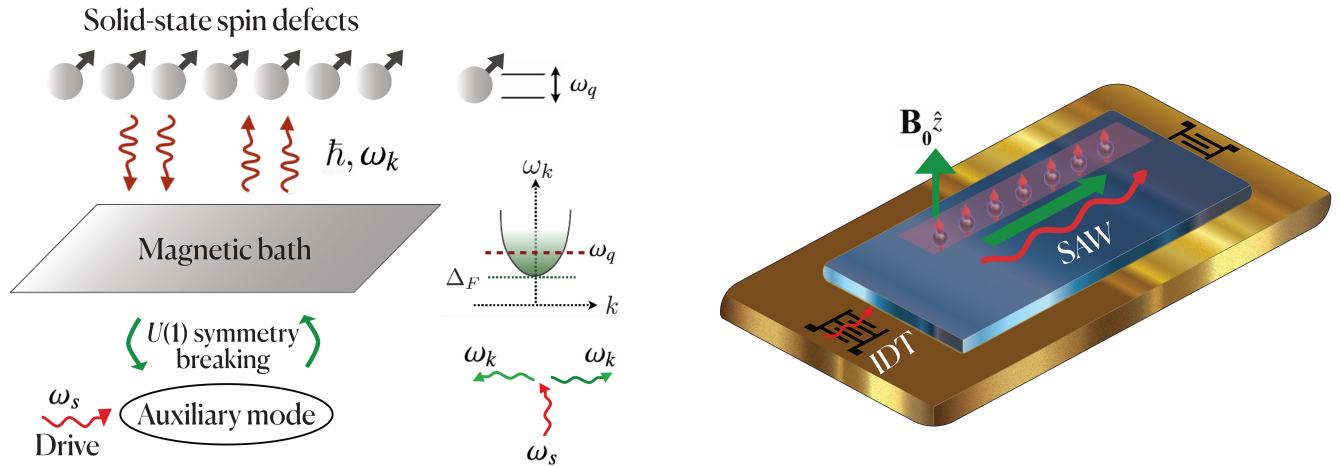


FIG. 1: Left: Schematic illustration of the proposed scheme for generating steady-state spin squeezing in an ensemble of solid-state spin defects interacting with a magnetic bath. A nonlinear,  $U(1)$ -symmetry breaking, interaction between the magnetic reservoir and an auxiliary mode, classically driven at frequency  $\omega_s$ , generates non-equilibrium squeezed states, i.e., correlated magnon pairs with frequency  $\omega_k \approx \omega_s/2$ , within the bath. When the resonance frequency  $\omega_q$  of the solid-state spin defects is tuned above the spin-wave gap  $\Delta_F$ , i.e.,  $\omega_q > \Delta_F$ , the ensemble can simultaneously absorb and emit correlated magnon pairs from and into the bath, which, in turn, facilitates the buildup of steady-state spin squeezing within the ensemble. Right: A possible realization of our scheme. An array of solid-state spin defects lies above a magnetic sample placed on top of a piezoelectric crystal. Two interdigital transducers (IDTs) generate SAWs that propagate through the crystal, periodically applying strain to the magnet. A static magnetic field  $\mathbf{B}_0$  aligns the magnetic order in the ferromagnetic bath along the  $\hat{z}$  direction.

formalism to non-stationary solid-state baths to then prove that, for magnetic reservoirs, the generation of spin squeezing relies on a time-dependent  $U(1)$ -symmetry-breaking mechanism. Our general recipe is summarized in Fig. 1. An ensemble of solid-state qubits with resonance frequency  $\omega_q$  interacts with a magnetic bath with spin-wave gap  $\Delta_F$  in the regime  $\omega_q > \Delta_F$ , which allows for the qubit and the bath to exchange energy, in the form of magnetic excitations, at the qubit resonance frequency. The magnetic bath is, in turn, coupled to an auxiliary mode via a nonlinear interaction that breaks its  $U(1)$ -symmetry. The auxiliary mode is driven classically at a frequency  $\omega_s \approx 2\omega_q$ . This nonlinear interaction generates entangled magnon pairs, which squeeze the bath modes, enabling the simultaneous emission and absorption of correlated magnon pairs between the ensemble and the magnetic bath. This process serves as the source for the generation of steady-state many-body entanglement within the array.

The wide array of magnonic and hybrid magnonic systems exhibiting nonlinearities presents numerous opportunities for implementing our scheme [64, 65]. In this work, to provide concrete estimates for near-future experiments, we consider the setup illustrated in Fig. 1: an ensemble of solid-state spin defects is positioned above a ferromagnetic thin film, which is placed on a piezoelectric substrate that generates surface acoustic waves (SAWs) when a voltage is applied. As shown by several experiments [66–70], a voltage-driven SAW can induce a periodical strain that couples to the magnetization dynamics of the bath via magneto-elastic interactions. Here, we find that the coupling of the magnetic bath to Love SAWs can induce effective magnon-magnon interactions that are formally analogous to the non-equilibrium two-mode squeezing

observed in nonlinear optical systems [71, 72]. These non-trivial bath correlations are then transferred to the qubit ensemble, resulting in squeezing dynamics that, for experimentally achievable system parameters, can be detected through collective spin quadrature measurements. Additionally, we show that further insights into the entanglement within the system could be gained by probing the relaxation dynamics of the ensemble. Our predictions pave the way for generating stable many-body entangled states within ensembles of solid-state spin defects, which, in turn, could enable the use of their unique properties in multi-qubit sensing schemes and logic operations.

This paper is organized as follows. In Sec. II, we introduce a general framework that describes the dynamics of a qubit array interacting with magnetic field fluctuations emitted by a non-stationary solid-state environment and identify the key ingredients for the generation of steady-state spin squeezing. In Sec. III, we outline a recipe for generating non-equilibrium spin squeezing in a magnetic bath to then focus on the concrete example of a SAW-driven Yttrium iron garnet (YIG) thin film. In Sec. IV, we show that the interaction of an ensemble of NV centers interacting with the bath introduced in Sec. III can generate steady-state spin squeezing with the ensemble. Finally, Sec. V we present our conclusion and an outlook.

## II. GENERAL FRAMEWORK

We set the stage for our work by deriving a theoretical framework that describes the dynamics of an array of solid-state defects, modelled as two-level systems, interacting with

the magnetic field  $\mathbf{B}$  generated by a shared, non-stationary solid-state bath. The Hamiltonian of the qubit array can be written as

$$H = -\frac{1}{2} \sum_{\alpha} \omega_q \sigma_{\alpha}^z - \tilde{\gamma} \sum_{\alpha} (B_{\alpha}^+ \sigma_{\alpha}^- + B_{\alpha}^- \sigma_{\alpha}^+ + B_{\alpha}^z \sigma_{\alpha}^z), \quad (1)$$

where  $\sigma_{\alpha}$ , with  $\sigma_{\alpha}^{\pm} = (\sigma_{\alpha}^x \pm i\sigma_{\alpha}^y)/2$ , labels the quantum spin with resonance frequency  $\omega_q$  and gyromagnetic ratio  $\tilde{\gamma}$  residing the site  $\mathbf{r}_{\alpha}$ . Here,  $B_{\alpha}^{\pm} = B_{\alpha}^x \pm iB_{\alpha}^y$  and  $B_{\alpha}^z$  are the components of the stray field interacting with the  $\alpha$ th quantum spin. The interactions between a solid-state spin defect and the field fluctuations of a nearby solid-state reservoir are much weaker than the characteristic energy scales of the individual systems, and the bath relaxation dynamics are taken to be much faster than those of the qubit ensemble. Thus, we can derive the dynamics of the density matrix  $\rho_s$  of the qubit array in the Born-Markov approximations [73] as

$$\frac{d\rho_s(t)}{dt} = -i[H_{eff}, \rho_s] + \mathcal{L}(\rho), \quad (2)$$

with

$$H_{eff} = \sum_{\alpha\beta} \sum_{\mu,\bar{\mu}} \sum_{\nu,\bar{\nu}} J_{\alpha\beta}^{\mu\nu} \sigma_{\alpha}^{\bar{\mu}} \sigma_{\beta}^{\bar{\nu}}, \quad (3)$$

$$\mathcal{L}(\rho) = \sum_{\alpha\beta} \sum_{\mu,\bar{\mu}} \sum_{\nu,\bar{\nu}} \Gamma_{\alpha\beta}^{\mu\nu} \left( \sigma_{\alpha}^{\bar{\mu}} \rho_s \sigma_{\beta}^{\bar{\nu}} - \frac{1}{2} \{ \sigma_{\alpha}^{\bar{\mu}} \sigma_{\beta}^{\bar{\nu}}, \rho_s \} \right), \quad (4)$$

where the sums over different indices are such that  $(\mu, \bar{\mu}), (\nu, \bar{\nu}) \in \{(+, -), (-, +), (z, z)\}$ . While Eqs. (2)-(4) are formally identical to the dynamics investigated in Ref. [62], here we generalize them to a non-stationary bath. The coefficients  $J_{\alpha\beta}^{\mu\nu}$  and  $\Gamma_{\alpha\beta}^{\mu\nu}$  are given in terms of the magnetic field correlations as

$$\frac{J_{\alpha\beta}^{\mu\nu}}{(i\tilde{\gamma}^2/2)} = \int_0^{\infty} d\tau \langle B_{\alpha}^{\mu}(t) B_{\beta}^{\nu}(t-\tau) \rangle e^{i(\omega_{\alpha}^{\mu} t + \omega_{\beta}^{\nu}(t-\tau))} - \int_0^{\infty} d\tau \langle B_{\alpha}^{\mu}(t-\tau) B_{\beta}^{\nu}(t) \rangle e^{i(\omega_{\beta}^{\nu} t + \omega_{\alpha}^{\mu}(t-\tau))}, \quad (5)$$

$$\frac{\Gamma_{\alpha\beta}^{\mu\nu}}{\tilde{\gamma}^2} = \int_0^{\infty} d\tau \langle B_{\alpha}^{\mu}(t) B_{\beta}^{\nu}(t-\tau) \rangle e^{i(\omega_{\alpha}^{\mu} t + \omega_{\beta}^{\nu}(t-\tau))} + \int_0^{\infty} d\tau \langle B_{\alpha}^{\mu}(t-\tau) B_{\beta}^{\nu}(t) \rangle e^{i(\omega_{\beta}^{\nu} t + \omega_{\alpha}^{\mu}(t-\tau))}, \quad (6)$$

where  $\omega_{\alpha\beta}^{\pm} = \pm\omega_q$ ,  $\omega_{\alpha\beta}^z = 0$ . For a stationary bath, i.e., for  $t \rightarrow 0$ , Eqs. (5) and (6) reduce, respectively, to the coherent and dissipative inter-qubit couplings derived in Ref. [62].

In this work, we specialize to a  $n$ -dimensional magnetically ordered reservoir whose local spin density  $\mathbf{s}(\mathbf{r})$  generates a magnetic stray field

$$\mathbf{B}_{\alpha} = \int d^n \mathbf{r} \mathcal{D}(\mathbf{r}_{\alpha}, \mathbf{r}) \mathbf{s}(\mathbf{r}), \quad (7)$$

where  $\mathcal{D}(\mathbf{r}_{\alpha}, \mathbf{r})$  is the tensorial magnetostatic Green function [74]. To simplify the analysis, here we assume that the equilibrium orientation of the spin density in the magnetic bath is

along  $\hat{z}$ . The transverse spin density fluctuations in the magnetic reservoir can be then mapped to the magnon creation, i.e.,  $m_{\mathbf{k}}^{\dagger}$ , and annihilation, i.e.,  $m_{\mathbf{k}}$ , operators, by invoking the Holstein-Primakoff transformation [75]. This allows us to rewrite the components of  $\mathbf{B}_{\alpha}$  in terms of the magnon operators as proportional to  $\int d^2 \mathbf{k} [a_{\mathbf{k}}(\mathbf{r}_{\alpha}) m_{\mathbf{k}} + b_{\mathbf{k}}(\mathbf{r}_{\alpha}) m_{\mathbf{k}}^{\dagger}]$ , where  $a_{\mathbf{k}}(\mathbf{r}_{\alpha})$  and  $b_{\mathbf{k}}(\mathbf{r}_{\alpha})$  are coefficients determined by the magnetostatic Green function<sup>1</sup>. As shown in Fig. 1, the qubit frequency is tuned above the spin-wave gap, i.e.,  $\omega_q > \Delta_F$ , allowing for the exchange of real particles between the qubits and the magnetic bath. On the other hand, in the regime where  $\omega_q < \Delta_F$ , the Lindbladian (4) vanishes, indicating that the interaction between qubits is mediated solely by virtual magnons.

In contrast to Ref. [62], here we consider a magnetic reservoir with broken  $U(1)$ -symmetry, which prevents us from neglecting number non-conserving correlations such as  $\langle m_{\mathbf{k}}(t) m_{\mathbf{k}}(t') \rangle$  and  $\langle m_{\mathbf{k}}^{\dagger}(t) m_{\mathbf{k}}^{\dagger}(t') \rangle$ . These correlations — indicative of squeezing in the reservoir — are essential for generating squeezed many-body dynamics in the qubit array. Namely, when  $\langle m_{\mathbf{k}}(t) m_{\mathbf{k}}(t') \rangle \propto e^{-i\omega_{\mathbf{k}}(t+t')}$ , inter-qubit squeezing interactions of the type

$$\frac{\Gamma_{\alpha\beta}^{++}}{(\tilde{\gamma}^2)} \propto \int_0^{\infty} d^2 \mathbf{k} f(\mathbf{k}) e^{-i(\omega_{\mathbf{k}} - \omega_q)2t} \delta(\omega_{\mathbf{k}} - \omega_q), \quad (8)$$

(and similarly its Hermitian conjugate  $\Gamma_{\alpha\beta}^{--}$ ) with  $f(\mathbf{k})$  governed by the magnetostatic Green functions, become stationary if the bath hosts a magnon mode whose dispersion  $\omega_{\mathbf{k}}$  can meet the condition  $\omega_{\mathbf{k}} = \omega_q$ . In this scenario, the Lindbladian (4) takes the following form :

$$\begin{aligned} \mathcal{L}(\rho) = & \sum_{\alpha\beta} \Gamma_{\alpha\beta}^{-+} \left( \sigma_{\alpha}^{-} \rho_s \sigma_{\beta}^{+} - \frac{1}{2} \{ \sigma_{\alpha}^{+} \sigma_{\beta}^{-}, \rho_s \} \right) \\ & + \sum_{\alpha\beta} \Gamma_{\alpha\beta}^{+-} \left( \sigma_{\alpha}^{+} \rho_s \sigma_{\beta}^{-} - \frac{1}{2} \{ \sigma_{\alpha}^{-} \sigma_{\beta}^{+}, \rho_s \} \right) \\ & + \sum_{\alpha\beta} \Gamma_{\alpha\beta}^{--} \left( \sigma_{\alpha}^{+} \rho_s \sigma_{\beta}^{+} - \frac{1}{2} \{ \sigma_{\alpha}^{+} \sigma_{\beta}^{+}, \rho_s \} \right) \\ & + \sum_{\alpha\beta} \Gamma_{\alpha\beta}^{++} \left( \sigma_{\alpha}^{-} \rho_s \sigma_{\beta}^{-} - \frac{1}{2} \{ \sigma_{\alpha}^{-} \sigma_{\beta}^{-}, \rho_s \} \right). \end{aligned} \quad (9)$$

Here,  $\Gamma_{\alpha\beta}^{+-}$  ( $\Gamma_{\alpha\beta}^{-+}$ ) parameterizes the correlated emission (absorption) of magnons from (by) the array for  $\alpha \neq \beta$ , while for  $\alpha = \beta$  they reduce to the single-qubit relaxation rates routinely measured in quantum sensing experiments [77, 78]. On the other hand, the inter-qubit couplings  $\Gamma_{\alpha\beta}^{++}$ ,  $\Gamma_{\alpha\beta}^{--}$ , which can be obtained from Eq. (5) under secular approximation [73], describe the simultaneous generation (and absorption) of a pair of magnons with energy  $\omega_{\mathbf{k}} = \omega_q$  into (from) the reservoir. This mechanism is known to lead to the asymmetric noise reduction and amplification in the collective spin quadratures,

<sup>1</sup> Here, we neglect the contributions corresponding to two-magnon noise, e.g.,  $s^z \propto m_{\mathbf{k}}^{\dagger} m_{\mathbf{k}}$ , since they are negligible when the qubit resonance frequency  $\omega_q$  can be tuned above the spin-wave gap  $\Delta_F$  [62, 76].

and, thus, the generation and stabilization of spin squeezed states in the array [41, 42, 52–54].

It is important to note that, in contrast, the Hamiltonian interaction terms of the form  $J_{\alpha\beta}^{++}$  (and similarly  $J_{\alpha\beta}^{--}$ ) have the following structure:

$$\frac{J_{\alpha\beta}^{++}}{(i\tilde{\gamma}^2/2)} = \int_0^\infty d\tau \langle B_\alpha^+(t)B_\beta^+(t-\tau) \rangle e^{i\omega_q(2t-\tau)} - \int_0^\infty d\tau \langle B_\alpha^+(t-\tau)B_\beta^+(t) \rangle e^{i\omega_q(2t-\tau)}, \quad (10)$$

where the time-dependent part of the correlations  $\langle B_\alpha^+(t)B_\beta^+(t') \rangle$  is given by  $e^{-i\omega_k(t+t')}$ . It is straightforward to see that the terms inside integral on the right-hand side (RHS) of Eq. (10) are identical, which implies  $J_{\alpha\beta}^{++} = J_{\alpha\beta}^{--} = 0$ . Furthermore, as discussed in detail in Ref. [62], the typical strength of XY exchange interactions ( $J_{\alpha\beta}^{+-}$ ,  $J_{\alpha\beta}^{-+}$ ) is considerably higher than that of Ising interactions ( $J_{\alpha\beta}^{zz}$ ), which allows us to rewrite Hamiltonian (3) as

$$H_{eff} = \sum_{\alpha \neq \beta} J_{\alpha\beta} \sigma_\alpha^+ \sigma_\beta^-, \quad (11)$$

with  $J_{\alpha\beta} = J_{\alpha\beta}^{+-} + J_{\alpha\beta}^{-+}$ . In the following Section, we will show how a nonlinear  $U(1)$ -symmetry breaking coupling of a magnetic bath to an auxiliary driven mode can be harnessed to generate the array dynamics described by Eqs. (9) and (11).

### III. SQUEEZED BATH

In the previous Section, we showed that the squeezing dynamics described by Eq. (9) can be generated by coupling a qubit ensemble to a common magnetic reservoir, whose squeezing factors in both quadratures can oscillate resonantly with the qubit resonance frequency  $\omega_q$ . A key resource for the generation of such non-stationary squeezing correlations in the bath is a nonlinear three-mode interaction of the form  $m_{\mathbf{k}}m_{\mathbf{k}'}c^\dagger + m_{\mathbf{k}}^\dagger m_{\mathbf{k}'}^\dagger c$ . When the mode  $c$  is strongly driven at frequency  $\omega_s$  with an undepleted classical field amplitude  $g$ , that is,  $c(t) = ge^{-i\omega_s t}$ , the interaction reduces to  $m_{\mathbf{k}}m_{\mathbf{k}'}g^* + m_{\mathbf{k}}^\dagger m_{\mathbf{k}'}^\dagger g$ , *viz.*, a two-mode squeezing interaction of modes  $m_{\mathbf{k}}$  and  $m_{\mathbf{k}'}$  with an effective interaction strength  $g$ . This leads to the spontaneous generation of entangled pairs of magnons. Essentially, a quasi-particle with frequency  $\omega_s$  is converted into two bath modes  $m_{\mathbf{k}}$  and  $m_{\mathbf{k}'}$ , with frequency  $\omega_k$  (where we assumed  $\omega_k = \omega_{k'}$ ), such that  $\omega_s = 2\omega_k$ , and with finite correlations of the type  $\langle m_{\mathbf{k}}(t)m_{\mathbf{k}'}(t') \rangle \propto e^{-i\omega_k(t+t')}$ . As noted in the previous Section, these correlations can stabilize the otherwise fast oscillating inter-qubit coupling  $\Gamma_{\alpha\beta}^{\pm\pm}$  (9), when there exists a  $\mathbf{k}$  such that  $\omega_k = \omega_q$ , which, in turn, enables the simultaneous exchange of entangled magnon pairs between the bath and the qubit array.

In the following, we demonstrate how the well-established experimental setup depicted in Fig. 1 can generate such interactions. Specifically, we consider a ferromagnetic thin film of thickness  $L$  mounted on top of a piezoelectric material whose

SAW modes can be excited by a remote interdigital transducer (IDT) at frequency  $\omega_s$  [66]. The Hamiltonian of the non-interacting ferromagnetic system is given by

$$H_F = \int d^2\mathbf{r} \left[ -J\mathbf{s}(\mathbf{r}) \cdot \nabla^2\mathbf{s}(\mathbf{r}) - A(\mathbf{s}(\mathbf{r}) \cdot \hat{z})^2 - \tilde{\gamma}\mathbf{B}_0 \cdot \hat{z} \right], \quad (12)$$

where  $J$  and  $A$  parameterize, respectively, the strength of the symmetric (Heisenberg-like) exchange interaction and the uniaxial anisotropy,  $\mathbf{B}_0$  is the applied static magnetic field, while  $\mathbf{s}(\mathbf{r})$  here denotes the surface spin density. The magnetic excitations are coupled to the elastic displacement via magnetoelastic interactions, which, for a cubic solid with lattice constant  $a_0$ , is given by

$$H_{int} = \frac{nL}{s^2} \int d^2\mathbf{r} \sum_{\alpha\beta} [B_{\alpha\beta}s_\alpha(\mathbf{r})s_\beta(\mathbf{r})]\epsilon_{\alpha\beta}. \quad (13)$$

Here,  $s$  is the saturation surface spin density,  $n = 1/a_0^3$ ,  $B_{\alpha\beta}$  are the magneto-elastic coupling strengths and  $\epsilon_{\alpha\beta}$  is the elastic strain defined as  $\epsilon_{\alpha\beta} = \frac{1}{2}\left(\frac{\partial u_\alpha}{\partial \beta} + \frac{\partial u_\beta}{\partial \alpha}\right)$ ,  $\alpha, \beta \in \{x, y, z\}$  where  $\mathbf{u}$  describes the displacement field of the SAW. In order to generate the target quadrature squeezing, we consider a Love SAW propagating along the  $\hat{x}$  direction with polarization along  $\hat{y}$ , as shown in Fig. 1. Since the typical experimental microwave drive powers can generate a displacement amplitude in the nanometer range [66] that is significantly larger than the femtometer domain of the SAW zero-point motion amplitude [79], one can describe the SAW as a classical displacement field with amplitude  $u_0$ , *i.e.*,  $u_y = u_0 \sin(kx - \omega_s t)$ . The only non-zero strain components of the Love SAW are  $\epsilon_{xy} = \epsilon_{yx} = \frac{1}{2}ku_0 \cos(kx - \omega_s t)$ .

Invoking the Holstein-Primakoff (HP) transformation [75], from Eqs. (12) and (13) we can recast the bath Hamiltonian  $H_{tot} = H_F + H_{int}$  as

$$H_{tot} = \int d^2\mathbf{k} \left[ \omega_k m_{\mathbf{k}}^\dagger m_{\mathbf{k}} + 2g \cos(\omega_s t) (m_{\mathbf{k}} m_{-\mathbf{k}} - m_{\mathbf{k}}^\dagger m_{-\mathbf{k}}^\dagger) \right], \quad (14)$$

where  $\omega_k = Dk^2 + 2As + \gamma B_0$  is the spin-wave dispersion,  $\gamma$  the gyromagnetic ratio,  $D = Js$  the spin stiffness,  $g = i\hbar^2 n^2 L^2 B_{xy} \epsilon_{xy} / s^2$  is the static amplitude of the classically-driven field and the bosonic operators  $m_{\mathbf{k}}$  obey the commutation relation  $[m_{\mathbf{k}}, m_{\mathbf{k}'}^\dagger] = (2\pi)^2 \delta^2(\mathbf{k} - \mathbf{k}')$ , where  $\delta^2(\mathbf{k} - \mathbf{k}')$  is the Dirac delta function. Generally, magnons interact with their phononic environment even in the absence of external drives [80]. However, in the setup we consider, the stationary magneto-elastic interactions are much weaker than the coupling to the classically-driven Love wave and can thus be safely neglected.

The second term on the RHS of Eq. (14) describes the conversion of a phonon with frequency  $\omega_s$  into two magnons with frequency  $\omega_k$  (and vice-versa), *i.e.*, a process that breaks the  $U(1)$ -symmetry of the isolated magnon reservoir. As a result, this interaction mediates a two-mode non-equilibrium squeezing that allows for the generation of a squeezed state formally analogous to the squeezed vacuum generated in an optical system through a nonlinear medium [71, 72]. This

non-equilibrium bath squeezing might be probed experimentally by measuring the quadrature of the collective spin in a direction perpendicular to the mean spin, similar to the techniques used in atomic ensembles [39, 40].

For a narrow range of  $\mathbf{k}$  centered around the value for which  $\omega_k = \omega_s/2$ , where  $\mathbf{k}$  lies within the band of modes exhibiting significant squeezing relative to the central  $\mathbf{k}$  mode, the zero-temperature magnon bath correlations can be written as

$$\langle m_{\mathbf{k}}(t)m_{\mathbf{k}'}(t') \rangle = (2\pi)^2 M_k e^{-i\omega_k(t+t')} \delta^2(\mathbf{k} + \mathbf{k}'), \quad (15)$$

$$\langle m_{\mathbf{k}}^\dagger(t)m_{\mathbf{k}'}^\dagger(t') \rangle = (2\pi)^2 M_k^* e^{i\omega_k(t+t')} \delta^2(\mathbf{k} + \mathbf{k}'), \quad (16)$$

$$\langle m_{\mathbf{k}}^\dagger(t)m_{\mathbf{k}'}(t') \rangle = (2\pi)^2 N_k e^{i\omega_k(t-t')} \delta^2(\mathbf{k} - \mathbf{k}'), \quad (17)$$

$$\langle m_{\mathbf{k}}(t)m_{\mathbf{k}'}^\dagger(t') \rangle = (2\pi)^2 (N_k + 1) e^{-i\omega_k(t-t')} \delta^2(\mathbf{k} - \mathbf{k}'), \quad (18)$$

where  $N_k = \sinh^2(r_k)$ ,  $M_k = \cosh(r_k) \sinh(r_k) e^{i\phi}$ ,  $\phi = -i \log(g/|g|)$ . The squeezing parameter  $r_k$ , for  $\omega_k \approx \omega_s/2$ , is given by  $r_{k_0} = \frac{1}{2} \operatorname{arctanh}(|g|/\bar{\Delta})$ , where  $\bar{\Delta}$  denotes the bandwidth of the squeezed vacuum. We work in the stable domain of system parameters, i.e.,  $|g| < \bar{\Delta}$  for which  $r_{k_0} \approx |g|/2\bar{\Delta}$ . At a finite temperature  $T$ , Eqs. (15)-(18) hold when setting  $N_k \rightarrow \sinh^2(r_k) + n_B(\omega_k, T) (\sinh^2(r_k) + \cosh^2(r_k))$  and  $M_k \rightarrow \cosh(r_k) \sinh(r_k) (2n_B(\omega_k, T) + 1)$  where  $n_B(\omega_k, T)$  denotes the Bose-Einstein distribution of thermal magnons. Here the magnon correlations (15) and (16) can stabilize the squeezing inter-qubit squeezing interactions, as shown by Eq. (8). Effectively, a phonon with frequency  $\omega_s$  generates a correlated pair of magnons at frequency  $\omega_k$ , resulting in squeezing correlations within the magnon bath. When the qubit system has a frequency  $\omega_q > \Delta_F$  such that  $\omega_q \approx \omega_s/2$ , these squeezing correlations are transmitted to the qubit array, as we show in detail in the next Section.

#### IV. STEADY-STATE SPIN SQUEEZING

We now focus on tailoring the master equation (2) with Lindbladian (9) and effective Hamiltonian (11) to describe an array of NV centers with lattice constant  $a$  interacting dissipatively with the non-equilibrium squeezed ferromagnetic reservoir introduced in Sec. III. An NV center is a spin-triplet system whose degeneracy of the  $m_s = \pm 1$  is lifted by the applied bias magnetic field  $B_0$ . In other words, each qubit can then be modelled as a two-level system with a frequency  $\omega_q = \Delta_0 - \tilde{\gamma}B_0$ , where  $\Delta_0 = 2.87$  GHz represents the zero-field splitting of the NV center. This approximation is valid as long as the thermal energy of the system is much less than the energy of the higher NV center transition, i.e.,  $k_B T \ll \Delta_0 + \tilde{\gamma}B_0$ , which is compatible with the quantum regime  $T \rightarrow 0$  we are working in. To guarantee the emergence of squeezing interactions  $\propto \Gamma_{\alpha\beta}^{\pm\pm}$ , we take the NV resonance frequency  $\omega_q$  to be within the magnon continuum, i.e.,  $\omega_q > \Delta_F$  and the SAW drive frequency is chosen to satisfy the frequency matching conditions, i.e.,  $\omega_s = 2\omega_q$ .

When the distance  $d$  between the NVs and the magnetic film is much smaller than the characteristic wavelength  $\lambda =$

$\sqrt{D/(\omega_0 - \Delta_F)}$ , the inter-qubit couplings can be written as

$$J_{\alpha\beta}/\nu = -\frac{\pi}{2} \frac{\omega_q - \Delta_F}{\Delta_0} Y_0(\rho_{\alpha\beta}/\lambda), \quad (19)$$

$$\Gamma_{\alpha\beta}^{+-}/\nu = \pi \frac{\omega_q - \Delta_F}{\Delta_0} N_{k_0} J_0(\rho_{\alpha\beta}/\lambda), \quad (20)$$

$$\Gamma_{\alpha\beta}^{--}/\nu = \pi \frac{\omega_q - \Delta_F}{\Delta_0} (N_{k_0} + 1) J_0(\rho_{\alpha\beta}/\lambda), \quad (21)$$

$$\Gamma_{\alpha\beta}^{++}/\nu = \pi \frac{\omega_q - \Delta_F}{\Delta_0} M_{k_0}^* J_0(\rho_{\alpha\beta}/\lambda), \quad (22)$$

$$\Gamma_{\alpha\beta}^{-+}/\nu = \pi \frac{\omega_q - \Delta_F}{\Delta_0} M_{k_0} J_0(\rho_{\alpha\beta}/\lambda). \quad (23)$$

Here,  $\rho_{\alpha\beta} = |\mathbf{r}_\alpha - \mathbf{r}_\beta|$  is the distance between the  $\alpha$ th and the  $\beta$ th quantum spins, and  $\nu = (\pi h^3 (\gamma\tilde{\gamma})^2 s \Delta_0 / D^2)$  is a characteristic frequency controlling the strength of the inter-qubit interactions. For concreteness, here we consider a YIG thin film with a thickness of  $L = 20$  nm,  $a_0 = 12.3$  Å,  $D = 5.1 \times 10^{-28}$  erg·cm<sup>2</sup>,  $s = 1.2 \times 10^{-10}$  G<sup>2</sup>·cm·s, zero field gap  $2A_s = 3.6 \times 10^{-18}$  erg·cm<sup>2</sup> and  $B_{xy} = 1988$  GHz [80, 81]. In order to realize an ensemble of qubits with long-range dissipative interactions, one needs to maximize  $\lambda$ , which can be achieved by minimizing  $\omega_0 - \Delta_F$ . For  $B_0 \approx 40$  mT, one finds  $\omega_q - \Delta_F \approx 100$  MHz, which implies  $\lambda \approx 277$  nm and  $\nu \approx 75$  Hz. The squeezing parameter  $r_{k_0}$  depends on the nonlinear interaction strength  $g$ , which, in turn, is a function of  $\epsilon_{xy}$  controlled by the power ( $P_{SAW}$ ) of the SAW drive, i.e.,  $\epsilon_{xy} \propto \sqrt{P_{SAW}}$ . For SAW drive powers close to 80 mW and velocity of the SAW  $\approx 3400$  m/s, one finds  $\epsilon_{xy} \approx 10^{-4}$  [66]. The corresponding nonlinear coupling strength of  $g \approx 0.1$  MHz can generate a squeezing  $r_{k_0} \approx 0.2$ , which yields  $N_{k_0} \approx 0.04$  and  $|M_{k_0}| \approx 0.2$ , where  $N_{k_0}$  represents the average magnon number at temperature  $T = 0$ . Figure 2 (a) shows the dependence of the coherent and dissipative inter-qubit interactions described by Eqs. (19)-(23) on the inter-qubit separation  $\rho_{\alpha\beta}$ . As one would expect, when  $r_k \rightarrow 0$ , Eqs. (20), (22), and (23) vanish, leaving only the interaction  $\Gamma_{\alpha\beta}^{+-}$  describing correlated emission, which is responsible for the emergence of superradiant and subradiant collective dynamics [62]. Given that  $N_{k_0} \ll 1$ , the magnitude of  $\Gamma_{\alpha\beta}^{+-}$  is much smaller than that of the other interaction terms. That is, the rate at which the NV array absorbs single magnons from the bath is considerably weaker than the rates at which it absorbs magnon pairs and emits both single magnons and magnon pairs into the bath. Nonetheless, the vacuum fluctuations of the bath can play a role analogous to that of a finite thermal magnon population in the emergence of superradiant and subradiant cooperative dynamics, as we discuss in detail later on. Finally, we note that the structure of the Lindbladian (9) with interaction terms given by Eqs. (20)-(23) is in one-to-one correspondence with squeezed vacuum reservoirs in quantum-optical systems [53, 73]. In analogy with the latter [73], we can introduce a jump operator  $C_\alpha = \cosh(r_{k_0})\sigma_\alpha^- + \sinh(r_{k_0})e^{i\phi}\sigma_\alpha^+$  that allows

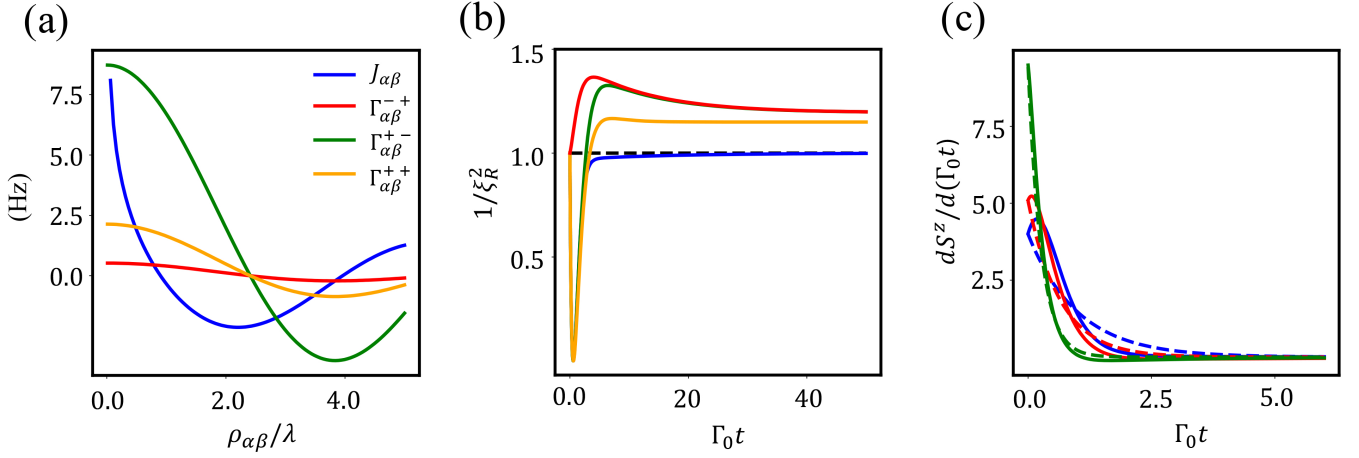


FIG. 2: (a) Dependence of the coherent and dissipative interqubit couplings defined in Eqs. (19)-(22) on the inter-qubit separation  $\rho_{\alpha\beta}$  (in units of the wavelength  $\lambda$ ). The parameters used are for the ensemble of NV-center spins interacting via a YIG thin film driven into a non-equilibrium squeezed state detailed in the main text. (b) Inverse of Wineland's squeezing parameter  $1/\xi_R^2$  as a function of time for  $N = 2$  NV centers. The blue and green curves correspond to the squeezing dynamics of an ensemble with lattice constant  $a/\lambda = 0.5$  initialized in the fully excited state with, respectively, squeezing parameter  $r_{k_0} = 0$  and  $r_{k_0} = 0.25$ , whereas the orange curve corresponds to an ensemble with lattice constant  $a/\lambda = 1$  and squeezing parameter  $r_{k_0} = 0.25$ . The red curve depicts the squeezing dynamics of the NV ensemble initialized in the ground state with squeezing parameter  $r_{k_0} = 0.25$  and lattice constant  $a/\lambda = 0.5$ . (c) The relaxation dynamics of  $N = 4$  NV centers are compared for a non-interacting ensemble (dotted lines with  $a/\lambda \gg 1$ ) and a correlated array (solid lines with lattice constant  $a/\lambda = 0.4$ ). The blue, red and green curves correspond to the squeezing parameter  $r_{k_0} = 0, 0.5, 1$ , respectively. (b,c) The time  $t$  is in units of the relaxation time  $\Gamma_0$  of an array of  $N$  noninteracting spin defects.

to recast the Linbladian (9) as

$$\mathcal{L}(\rho) = \pi \frac{\omega_q - \Delta_F}{\Delta_0} \sum_{\alpha,\beta} J_0(\rho_{\alpha\beta}/\lambda) \left[ \frac{1}{2} \{ C_\alpha^\dagger C_\beta, \rho_s \} - C_\alpha \rho_s C_\beta^\dagger \right], \quad (24)$$

which ensures that the system decays into the Gibbs ensemble in the long-time limit, showcasing stable spin squeezing.

We proceed to explore the generation of steady-state spin squeezing in an array of  $N$  qubits whose dynamics is described by Eqs. (9) and (11), with coherent and dissipative exchange interactions given by Eqs. (19)-(23). We quantify the degree of spin squeezing via the Wineland squeezing parameter  $\xi_R^2$  [33], which is defined as

$$\xi_R^2 = N \frac{\langle \Delta \mathbf{S}_\perp^2 \rangle}{\langle \mathbf{S} \rangle^2}, \quad (25)$$

where  $\langle \Delta \mathbf{S}_\perp^2 \rangle$  denotes the minimum variance in the plane perpendicular to the mean spin direction and the collective spin operators are defined as  $S^\alpha = \sum_{i=1}^N \sigma_i^\alpha$ ,  $\alpha \in \{x, y, z\}$ . A value of  $\xi_R^2 < 1$  signifies that the collective spin states are squeezed, indicating a suppression of noise below the standard quantum limit and, in the case of an ensemble of spin-1/2 particles, a finite multipartite entanglement [5].

We start our analysis by numerically simulating the dynamics of the system for  $N = 2$  qubits. We use a scaled time  $\Gamma_0 t$  to simulate the system's time evolution, where  $\Gamma_0 \approx 8.2$  Hz, corresponding to  $\Gamma_{\alpha\alpha}^{+-}$  in Eq. (21), represents the relaxation rate of an isolated NV center interacting solely with the magnetic

bath. Figure 2(b) shows the temporal evolution of the spin squeezing parameter (25) for squeezing parameter  $r_{k_0} = 0, 0.25$ , and array lattice constant  $a/\lambda = 0.5, 1$ . As expected, when the system is initialized in the excited state, for  $r_{k_0} = 0$ ,  $a/\lambda = 0.5$ , we observe  $1/\xi_R^2 \rightarrow 1$  in the long-time limit (blue curve). That is, the system does not exhibit any squeezing when the bath is not driven into a squeezed state. In contrast, for  $r_{k_0} = 0.25$  and  $a/\lambda = 0.5$ , we find that the two qubits reach an entangled steady-state, i.e.,  $1/\xi_R^2 > 1$  in the long-time limit (green curve). As  $a/\lambda$  increases, the strength of the inter-qubit interaction diminishes, resulting in weaker steady-state squeezing, as seen by comparing the long-term dynamics of the orange curve in Fig. 2(b).

The red curve in Fig. 2(b) represents the plot of  $1/\xi_R^2$  as a function of time with the squeezing parameter  $r_{k_0} = 0.25$ ,  $a/\lambda = 0.5$  when the ensemble is initialized in the ground state. Unlike the all-excited state,  $1/\xi_R^2 > 1$  for the all-down state at all times. The apparent discrepancy in the short-time evolution of spin squeezing between the green and red curves arises from the difference in initial conditions: the ensemble is initialized in the all-excited state for the green curve and in the ground state for the red curve. We find that the ensemble initialized in the ground state rapidly evolves into a squeezed state due to its interaction with the bath, to then display finite spin squeezing  $1/\xi_R^2 > 1$  at all later times. Conversely, the short-time dynamics of the ensemble initialized in the fully excited state suggest that it undergoes superradiant decay into a squeezed environment before exhibiting spin squeezing. We have also verified that, when all other parameters are identi-

cal, the ensembles exhibit the same degree of spin squeezing in the long-time limit, i.e., they evolve to a unique steady spin-squeezed state independent of their initialization.

In Fig. 2(c), we plot the time evolution of the collective relaxation rate for an array of  $N = 4$  qubits initialized in the excited state, with varying  $r_{k_0}$ . In the absence of squeezing ( $r_{k_0} = 0$ ), the collective relaxation rate of a correlated ensemble (solid blue line) displays a superradiant burst followed by a subradiant tail, in contrast to the exponentially decaying dynamics of an uncorrelated ensemble of the same size (dashed blue line). However, as the squeezing parameter  $r_{k_0}$  increases and the bath becomes more populated, the superradiant and subradiant behaviours are suppressed, ultimately leading to collective relaxation dynamics nearly identical to that of an uncorrelated ensemble when  $r_{k_0} = 1$  characterized by the merging of the solid and dotted green lines. This observation suggests that the relaxation dynamics of a correlated ensemble could serve as a qualitative indicator of the presence or absence of squeezing in the reservoir. For instance, in the setup we consider, non-equilibrium squeezing in the bath could be detected by probing the relative suppression or amplification of superradiant and subradiant dynamics when the SAW voltage drive is switched, respectively, on or off.

## V. CONCLUSIONS

In this work, we develop a theoretical framework that captures the many-body quantum dynamics of a spin qubit array interacting with electromagnetic noise emitted by a non-stationary magnetic bath. We find that a key ingredient for generating steady-state spin squeezing within the ensemble is a magnetic reservoir hosting non-equilibrium squeezed

states consisting of magnon pairs at the qubit resonance frequency. The latter can be generated through a nonlinear,  $U(1)$ -symmetry-breaking interaction between the magnons and an auxiliary mode: we show it explicitly by focusing on a ferromagnetic thin film coupled to classically driven surface acoustic waves (SAWs). We investigate the many-body dynamics of an ensemble of NV centers interacting with the driven YIG reservoir and show that, within experimentally feasible parameters, the bath-qubit coupling can drive the ensemble into a steady-state spin squeezed state. The presence of steady-state spin squeezing, which can be switched on and off via voltage, can be probed through measurements of the collective spin states of the ensemble, without the need for individual qubit addressability.

While our work specializes on a concrete setup to provide guidance for near-term experiments, it more broadly paves the way for engineering entanglement in ensembles of solid-state defects through the largely unexplored approach of reservoir engineering in solid-state baths. The broad spectrum of non-equilibrium driving knobs and of nonlinear interactions between magnons and various physical platforms unlocks a wide array of possibilities for implementing our proposal [64, 65, 82]. Such tunability is a distinctive feature of solid-state reservoirs, offering unique opportunities to engineer and explore non-classical properties and structured dissipation in far-from-equilibrium baths that cannot be seamlessly replicated in quantum optical setups.

## VI. ACKNOWLEDGEMENTS

The authors thank A. A. Garcia, A. Clerk, L. Viola, G. S. Agarwal and V. Flynn for helpful discussions, and acknowledge support from DOE under Award No. DE-SC0024090.

- 
- [1] C. Orzel, A. Tuchman, M. Fenselau, M. Yasuda, and M. Kasevich, Squeezed states in a bose-einstein condensate, *Science* **291**, 2386 (2001).
  - [2] J. Esteve, C. Gross, A. Weller, S. Giovanazzi, and M. K. Oberthaler, Squeezing and entanglement in a bose-einstein condensate, *Nature* **455**, 1216 (2008).
  - [3] C. Gross, T. Zibold, E. Nicklas, J. Esteve, and M. K. Oberthaler, Nonlinear atom interferometer surpasses classical precision limit, *Nature* **464**, 1165 (2010).
  - [4] M. F. Riedel, P. Böhi, Y. Li, T. W. Hänsch, A. Sinatra, and P. Treutlein, Atom-chip-based generation of entanglement for quantum metrology, *Nature* **464**, 1170 (2010).
  - [5] A. Sørensen, L.-M. Duan, J. I. Cirac, and P. Zoller, Many-particle entanglement with bose-einstein condensates, *Nature* **409**, 63 (2001).
  - [6] C. Law, H. Ng, and P. Leung, Coherent control of spin squeezing, *Physical Review A* **63**, 055601 (2001).
  - [7] U. V. Poulsen and K. Mølmer, Positive-p simulations of spin squeezing in a two-component bose condensate, *Physical Review A* **64**, 013616 (2001).
  - [8] S. Raghavan, H. Pu, P. Meystre, and N. Bigelow, Generation of arbitrary dicke states in spinor bose-einstein condensates, *Optics communications* **188**, 149 (2001).
  - [9] S. D. Jenkins and T. B. Kennedy, Spin squeezing in a driven bose-einstein condensate, *Physical Review A* **66**, 043621 (2002).
  - [10] D. Jaksch, J. I. Cirac, and P. Zoller, Dynamically turning off interactions in a two-component condensate, *Physical Review A* **65**, 033625 (2002).
  - [11] H. Jing, Mutual coherence and spin squeezing in double-well atomic condensates, *Physics Letters A* **306**, 91 (2002).
  - [12] A. S. Sørensen, Bogoliubov theory of entanglement in a bose-einstein condensate, *Physical Review A* **65**, 043610 (2002).
  - [13] A. Micheli, D. Jaksch, J. I. Cirac, and P. Zoller, Many-particle entanglement in two-component bose-einstein condensates, *Physical Review A* **67**, 013607 (2003).
  - [14] K. Mølmer, Quantum atom optics with bose-einstein condensates, *New Journal of Physics* **5**, 55 (2003).
  - [15] X.-Y. Lü, J.-Q. Liao, L. Tian, and F. Nori, Steady-state mechanical squeezing in an optomechanical system via duffing nonlinearity, *Phys. Rev. A* **91**, 013834 (2015).
  - [16] E. E. Wollman, C. Lei, A. Weinstein, J. Suh, A. Kronwald, F. Marquardt, A. A. Clerk, and K. Schwab, Quantum squeezing of motion in a mechanical resonator, *Science* **349**, 952 (2015).

- [17] A. Nunnenkamp, K. Børkje, J. Harris, and S. Girvin, Cooling and squeezing via quadratic optomechanical coupling, *Physical Review A—Atomic, Molecular, and Optical Physics* **82**, 021806 (2010).
- [18] T. P. Purdy, P.-L. Yu, R. W. Peterson, N. S. Kampel, and C. A. Regal, Strong optomechanical squeezing of light, *Physical Review X* **3**, 031012 (2013).
- [19] G. Agarwal and S. Huang, Strong mechanical squeezing and its detection, *Physical Review A* **93**, 043844 (2016).
- [20] S. Marti, U. von Lüpke, O. Joshi, Y. Yang, M. Bild, A. Omannen, Y. Chu, and M. Fadel, Quantum squeezing in a nonlinear mechanical oscillator, *Nature Physics*, 1 (2024).
- [21] A. Szorkovszky, A. C. Doherty, G. I. Harris, and W. P. Bowen, Mechanical squeezing via parametric amplification and weak measurement, *Phys. Rev. Lett.* **107**, 213603 (2011).
- [22] A. Kamra, W. Belzig, and A. Brataas, Magnon-squeezing as a niche of quantum magnonics, *Applied Physics Letters* **117** (2020).
- [23] J. Li, S.-Y. Zhu, and G. Agarwal, Squeezed states of magnons and phonons in cavity magnomechanics, *Physical Review A* **99**, 021801 (2019).
- [24] A. Kamra and W. Belzig, Super-poissonian shot noise of squeezed-magnon mediated spin transport, *Phys. Rev. Lett.* **116**, 146601 (2016).
- [25] A. Kamra, U. Agrawal, and W. Belzig, Noninteger-spin magnonic excitations in untextured magnets, *Phys. Rev. B* **96**, 020411 (2017).
- [26] A. Kamra, E. Thingstad, G. Rastelli, R. A. Duine, A. Brataas, W. Belzig, and A. Sudbø, Antiferromagnetic magnons as highly squeezed fock states underlying quantum correlations, *Phys. Rev. B* **100**, 174407 (2019).
- [27] J. Zou, S. K. Kim, and Y. Tserkovnyak, Tuning entanglement by squeezing magnons in anisotropic magnets, *Phys. Rev. B* **101**, 014416 (2020).
- [28] J. Ma, X. Wang, C.-P. Sun, and F. Nori, Quantum spin squeezing, *Physics Reports* **509**, 89 (2011).
- [29] A. Kuzmich, K. Mølmer, and E. Polzik, Spin squeezing in an ensemble of atoms illuminated with squeezed light, *Physical review letters* **79**, 4782 (1997).
- [30] J. Appel, P. J. Windpassinger, D. Oblak, U. B. Hoff, N. Kjaergaard, and E. S. Polzik, Mesoscopic atomic entanglement for precision measurements beyond the standard quantum limit, *Proceedings of the National Academy of Sciences* **106**, 10960 (2009).
- [31] A. Louchet-Chauvet, J. Appel, J. J. Renema, D. Oblak, N. Kjaergaard, and E. S. Polzik, Entanglement-assisted atomic clock beyond the projection noise limit, *New Journal of Physics* **12**, 065032 (2010).
- [32] T. Takano, M. Fuyama, R. Namiki, and Y. Takahashi, Spin squeezing of a cold atomic ensemble with the nuclear spin of one-half, *Physical review letters* **102**, 033601 (2009).
- [33] D. J. Wineland, J. J. Bollinger, W. M. Itano, F. Moore, and D. J. Heinzen, Spin squeezing and reduced quantum noise in spectroscopy, *Physical Review A* **46**, R6797 (1992).
- [34] D. J. Wineland, J. J. Bollinger, W. M. Itano, and D. J. Heinzen, Squeezed atomic states and projection noise in spectroscopy, *Physical Review A* **50**, 67 (1994).
- [35] N. Bigelow, Squeezing entanglement, *Nature* **409**, 27 (2001).
- [36] M. Kitagawa and M. Ueda, Squeezed spin states, *Phys. Rev. A* **47**, 5138 (1993).
- [37] E. Davis, G. Bentsen, and M. Schleier-Smith, Approaching the heisenberg limit without single-particle detection, *Phys. Rev. Lett.* **116**, 053601 (2016).
- [38] A. Chu, P. He, J. K. Thompson, and A. M. Rey, Quantum enhanced cavity qed interferometer with partially delocalized atoms in lattices, *Phys. Rev. Lett.* **127**, 210401 (2021).
- [39] O. Hosten, R. Krishnakumar, N. J. Engelsen, and M. A. Kasevich, Quantum phase magnification, *Science* **352**, 1552 (2016).
- [40] I. D. Leroux, M. H. Schleier-Smith, and V. Vuletić, Implementation of cavity squeezing of a collective atomic spin, *Physical Review Letters* **104**, 073602 (2010).
- [41] E. G. Dalla Torre, J. Otterbach, E. Demler, V. Vuletic, and M. D. Lukin, Dissipative preparation of spin squeezed atomic ensembles in a steady state, *Phys. Rev. Lett.* **110**, 120402 (2013).
- [42] P. Groszkowski, M. Koppenhöfer, H.-K. Lau, and A. A. Clerk, Reservoir-engineered spin squeezing: Macroscopic even-odd effects and hybrid-systems implementations, *Phys. Rev. X* **12**, 011015 (2022).
- [43] K. Seetharam, A. Lerose, R. Fazio, and J. Marino, Correlation engineering via nonlocal dissipation, *Phys. Rev. Res.* **4**, 013089 (2022).
- [44] J. I. Cirac, A. S. Parkins, R. Blatt, and P. Zoller, “dark” squeezed states of the motion of a trapped ion, *Phys. Rev. Lett.* **70**, 556 (1993).
- [45] A. Kronwald, F. Marquardt, and A. A. Clerk, Arbitrarily large steady-state bosonic squeezing via dissipation, *Phys. Rev. A* **88**, 063833 (2013).
- [46] N. Didier, F. Qassemi, and A. Blais, Perfect squeezing by damping modulation in circuit quantum electrodynamics, *Phys. Rev. A* **89**, 013820 (2014).
- [47] D. Kienzler, H.-Y. Lo, B. Keitch, L. De Clercq, F. Leupold, F. Lindenfesler, M. Marinelli, V. Negnevitsky, and J. Home, Quantum harmonic oscillator state synthesis by reservoir engineering, *Science* **347**, 53 (2015).
- [48] F. Lecocq, J. B. Clark, R. W. Simmonds, J. Aumentado, and J. D. Teufel, Quantum nondemolition measurement of a nonclassical state of a massive object, *Phys. Rev. X* **5**, 041037 (2015).
- [49] J.-M. Pirkkalainen, E. Damskägg, M. Brandt, F. Massel, and M. A. Sillanpää, Squeezing of quantum noise of motion in a micro-mechanical resonator, *Phys. Rev. Lett.* **115**, 243601 (2015).
- [50] C. U. Lei, A. J. Weinstein, J. Suh, E. E. Wollman, A. Kronwald, F. Marquardt, A. A. Clerk, and K. C. Schwab, Quantum nondemolition measurement of a quantum squeezed state beyond the 3 db limit, *Phys. Rev. Lett.* **117**, 100801 (2016).
- [51] R. Dassonneville, R. Assouly, T. Peronnin, A. Clerk, A. Bienfait, and B. Huard, Dissipative stabilization of squeezing beyond 3 db in a microwave mode, *PRX Quantum* **2**, 020323 (2021).
- [52] G. Agarwal and R. Puri, Nonequilibrium phase transitions in a squeezed cavity and the generation of spin states satisfying uncertainty equality, *Optics communications* **69**, 267 (1989).
- [53] G. S. Agarwal and R. R. Puri, Cooperative behavior of atoms irradiated by broadband squeezed light, *Phys. Rev. A* **41**, 3782 (1990).
- [54] G. S. Agarwal and R. R. Puri, Atomic states with spectroscopic squeezing, *Phys. Rev. A* **49**, 4968 (1994).
- [55] T. Gaebel, M. Domhan, I. Popa, C. Wittmann, P. Neumann, F. Jelezko, J. R. Rabreau, N. Stavrias, A. D. Greentree, S. Praver, *et al.*, Room-temperature coherent coupling of single spins in diamond, *Nature Physics* **2**, 408 (2006).
- [56] A. Bermudez, F. Jelezko, M. B. Plenio, and A. Retzker, Electron-mediated nuclear-spin interactions between distant nitrogen-vacancy centers, *Phys. Rev. Lett.* **107**, 150503 (2011).
- [57] F. Dolde, I. Jakobi, B. Naydenov, N. Zhao, S. Pezzagna, C. Trautmann, J. Meijer, P. Neumann, F. Jelezko, and J. Wrachtrup, Room-temperature entanglement between single



- defect spins in diamond, *Nature Physics* **9**, 139 (2013).
- [58] L. Trifunovic, F. L. Pedrocchi, and D. Loss, Long-distance entanglement of spin qubits via ferromagnet, *Phys. Rev. X* **3**, 041023 (2013).
- [59] B. Flebus and Y. Tserkovnyak, Entangling distant spin qubits via a magnetic domain wall, *Phys. Rev. B* **99**, 140403 (2019).
- [60] M. Fukami, D. R. Candido, D. D. Awschalom, and M. E. Flatté, Opportunities for long-range magnon-mediated entanglement of spin qubits via on- and off-resonant coupling, *PRX Quantum* **2**, 040314 (2021).
- [61] P. Andrich, C. F. de las Casas, X. Liu, H. L. Bretscher, J. R. Berman, F. J. Heremans, P. F. Nealey, and D. D. Awschalom, Long-range spin wave mediated control of defect qubits in nanodiamonds, *npj Quantum Information* **3**, 28 (2017).
- [62] X. Li, J. Marino, D. E. Chang, and B. Flebus, A solid-state platform for cooperative quantum phenomena, arXiv preprint arXiv:2309.08991 (2023).
- [63] M. Reitz, C. Sommer, and C. Genes, Cooperative quantum phenomena in light-matter platforms, *PRX Quantum* **3**, 010201 (2022).
- [64] B. Flebus, Magnonics in collinear magnetic insulating systems, *Journal of Applied Physics* **129** (2021).
- [65] S. Zheng, Z. Wang, Y. Wang, F. Sun, Q. He, P. Yan, and H. Yuan, Tutorial: nonlinear magnonics, *Journal of Applied Physics* **134** (2023).
- [66] L. Dreher, M. Weiler, M. Pernpeintner, H. Huebl, R. Gross, M. S. Brandt, and S. T. B. Goennenwein, Surface acoustic wave driven ferromagnetic resonance in nickel thin films: Theory and experiment, *Phys. Rev. B* **86**, 134415 (2012).
- [67] M. Weiler, L. Dreher, C. Heeg, H. Huebl, R. Gross, M. S. Brandt, and S. T. B. Goennenwein, Elastically driven ferromagnetic resonance in nickel thin films, *Phys. Rev. Lett.* **106**, 117601 (2011).
- [68] M. Xu, K. Yamamoto, J. Puebla, K. Baumgaertl, B. Rana, K. Miura, H. Takahashi, D. Grundler, S. Maekawa, and Y. Otani, Nonreciprocal surface acoustic wave propagation via magneto-rotation coupling, *Science advances* **6**, eabb1724 (2020).
- [69] M. Weiler, H. Huebl, F. S. Goerg, F. D. Czeschka, R. Gross, and S. T. B. Goennenwein, Spin pumping with coherent elastic waves, *Phys. Rev. Lett.* **108**, 176601 (2012).
- [70] S. Maekawa and M. Tachiki, Surface acoustic attenuation due to surface spin wave in ferro- and antiferromagnets, in *AIP Conference Proceedings*, Vol. 29 (American Institute of Physics, 1976) pp. 542–543.
- [71] R. W. Boyd, A. L. Gaeta, and E. Giese, Nonlinear optics, in *Springer Handbook of Atomic, Molecular, and Optical Physics* (Springer, 2008) pp. 1097–1110.
- [72] M. O. Scully and M. S. Zubairy, *Quantum optics* (Cambridge university press, 1997).
- [73] H.-P. Breuer and F. Petruccione, *The theory of open quantum systems* (Oxford University Press, USA, 2002).
- [74] K. Y. Guslienko and A. N. Slavin, Magnetostatic green's functions for the description of spin waves in finite rectangular magnetic dots and stripes, *Journal of magnetism and magnetic materials* **323**, 2418 (2011).
- [75] T. Holstein and H. Primakoff, Field dependence of the intrinsic domain magnetization of a ferromagnet, *Physical Review* **58**, 1098 (1940).
- [76] B. Flebus and Y. Tserkovnyak, Quantum-impurity relaxometry of magnetization dynamics, *Phys. Rev. Lett.* **121**, 187204 (2018).
- [77] C. Du, T. Van der Sar, T. X. Zhou, P. Upadhyaya, F. Casola, H. Zhang, M. C. Onbasli, C. A. Ross, R. L. Walsworth, Y. Tserkovnyak, *et al.*, Control and local measurement of the spin chemical potential in a magnetic insulator, *Science* **357**, 195 (2017).
- [78] H. Wang, S. Zhang, N. J. McLaughlin, B. Flebus, M. Huang, Y. Xiao, C. Liu, M. Wu, E. E. Fullerton, Y. Tserkovnyak, *et al.*, Noninvasive measurements of spin transport properties of an antiferromagnetic insulator, *Science advances* **8**, eabg8562 (2022).
- [79] M. J. A. Schuetz, E. M. Kessler, G. Giedke, L. M. K. Vandersypen, M. D. Lukin, and J. I. Cirac, Universal quantum transducers based on surface acoustic waves, *Phys. Rev. X* **5**, 031031 (2015).
- [80] B. Flebus, K. Shen, T. Kikkawa, K.-i. Uchida, Z. Qiu, E. Saitoh, R. A. Duine, and G. E. W. Bauer, Magnon-polaron transport in magnetic insulators, *Phys. Rev. B* **95**, 144420 (2017).
- [81] A. G. Gurevich and G. A. Melkov, *Magnetization oscillations and waves* (CRC press, 2020).
- [82] B. Flebus, D. Grundler, B. Rana, Y. Otani, I. Barsukov, A. Barman, G. Gubbiotti, P. Landeros, J. Akerman, U. Ebels, *et al.*, The 2024 magnonics roadmap, *Journal of Physics: Condensed Matter* **36**, 363501 (2024).